JIAYAN LI*,**, LIANG WANG*,**, JIANJIE HAO*,**, PING NI*,**, YI TAN*,**

THE CONTINUOUS GROWTH OF BULK Si BY TEMPERATURE GRADIENT ZONE MELTING METHOD

Temperature gradient zone melting (TGZM) method was used to obtain bulk Si continuously for the efficient separation and purification of primary Si from the Si-Al alloy in this work. The effects of alloy thickness, temperature gradient and holding time in TGZM purification technology were investigated. Finally, the continuous growth of bulk Si without eutectic inclusions was obtained. The results showed that the growth rate of bulk Si was independent of the liquid zone thickness. When the temperature gradient was changed from 2.48 K/mm to 3.97 K/mm, the growth rate of bulk Si was enhanced from 7.9×10^{-5} mm/s to 2.47×10^{-4} mm/s, which was increased by about 3 times. The bulk Si could grow continuously and the growth rate was decreased with the increase of holding time from 1 h to 5 h. Meanwhile, low refining temperature was beneficial to the removal of impurities. With a precipitation temperature of 1460 K and a temperature gradient of 2.48 K/mm, the removal rates of Fe, P and B were 99.8%, 94.0% and 63.6%, respectively.

Keywords: Bulk Si; TGZM; Si-Al alloy; Growth rate; Impurities

1. Introduction

As a high efficiency purification method of metallurgical silicon, solidification refining approach has been paid special attention at both domestic and overseas [1-5]. Therefore, Si-Al alloy refining is widely investigated as a low temperature purification method for the removal of the B, P and metal impurities by segregation effect [6-9]. Hypereutectic Si-Al alloys are used as the purification system. With the temperature decrease, silicon precipitates from the supersaturated Si-Al melting initially and the impurities are enriched in the liquid alloy melt due to the segregation behavior. It was reported that the segregation coefficient of boron between solid silicon and Si-Al alloy melt will reduce with the decrease of primary Si the precipitate temperature [10-12]. The primary Si was distributed homogeneously in the whole alloy ingot under uniform temperature field and the acid etching was required to remove the Al and recycle high purity Si [13,14]. The electromagnetic stirring [15,16], electric currents [17], super gravity [18,19], centrifugal technologies [20] and solidification under the temperature gradient [21] were investigated during recycling process. Recently, the Morita group proposed a bulk Si growth method by directional solidification. The high-quality bulk Si can be obtained from Si-Al [22], and Si-Sn [23-24], respectively. The effects of the diffusion of Si in the melt on the crystal growth were studied in that work. The growth of bulk Si from the Si-Al eutectic structure is particularly beneficial to the recycling of high purifying Si.

TGZM is a traditional method, which is usually used to grow perfect crystals, electrically heterogeneous structures and epitaxial layers of semiconductor, as well as applying to physico-chemical investigation [25,26]. In previous study [27], some basic work was conducted in our group and has demonstrated that the TGZM approach could apply to alloy solidification refining process for the bulk Si growth from the Si-Al alloy by adding additional Si source. The Si source dissolved at the hot side, Si atoms diffused in alloy melt and the bulk Si also precipitated and grew successively at the bottom cold side. The SiC phase interface with approximately 10 μm thickness was obtained between the bulk Si and the graphite crucible wall and the rough interface of graphite crucible will be beneficial for the growth of bulk Si. The primary Si could separate successfully from the eutectic substrate.

In this paper, the effects of alloy thickness, holding time and temperature gradient on the growth of bulk Si were investigated in detail respectively. Meanwhile, the morphology of bulk Si, the growth rates and the distribution of impurities were analyzed. Ultimately, the influence factors and experimental conditions for the growth stabilization of bulk Si in Si-Al alloy through TGZM method were obtained.

2. Experimental

Firstly, alloys with a composition of 65 mol.% Si-Al (99.99% purity Al and 98% purity MG-Si) were casted into

* DALIAN UNIVERSITY OF TECHNOLOGY, SCHOOL OF MATERIALS SCIENCE AND ENGINEERING, DALIAN 116024, CHINA
** DALIAN UNIVERSITY OF TECHNOLOGY, KEY LABORATORY FOR SOLAR ENERGY PHOTOVOLTAIC SYSTEM OF LIAONING PROVINCE, DALIAN 116024, CHINA

Corresponding author: lijiayan@dlut.edu.cn

cylindrical rods of 10 mm diameter with an air cooling rate by a super-audio induction heating furnace. The alloy was cut into different thickness. The MG-Si ingot (98% purity) was grinded and polished into cylindrical rods with 10 mm diameter and 17 mm length as the Si source. Then, the alloy and Si source were put into a high purity graphite crucible which was placed in a heating furnace with a temperature gradient. The control technique about temperature gradient was described in previous paper [27]. Argon atmosphere was used to protect the samples from oxidation. The temperature gradient was changed by setting different heating temperature. In this work, the heating temperatures were set at 1473 K, 1573 K and 1673 K, respectively. Si source was added at the hot side and the alloy was placed at the cold side. Finally, the samples were took out from the furnace and cooled to room temperature in the air when the experiments ended.

After the TGZM process, the Si-Al alloy samples were cut into two parts. One part was carefully polished and used for the macro morphologies analysis by the Microtek Scanmaker (i360, Shanghai, China). The impurities contents and the inclusion distribution in primary Si were detected by an inductively coupled plasma mass spectrometer (ICP-MS, Qingdao, China) and the electron probe microanalysis (EPMA-1600, Shimadzu, Japan), respectively.

3. Results and discussions

3.1. The growth regularities in TGZM

The TGZM schematic diagram was shown in Fig. 1. The Si source was placed on the top of Si-Al alloy, which was considered as an ensemble and placed in a temperature gradient. When a positive temperature gradient was applied, the Si concentration gradient was formed in the alloy melt due to the Si source dissolution. Gradually, the bulk Si began to grow at the underneath of liquid alloy melt with a low temperature according to the solute transportation. Further, the growth rate was related with the atomic kinetics of the interface reactions and the equation for the growth rate can be written as following [28]:

$$V = \mu \Delta T = m\mu \Delta C \qquad (1)$$

Where V is the average growth velocity perpendicular to the solid-liquid interface, μ is an atomic coefficient (usually, $10 < \mu < 10^4$ mm/s·K). ΔT is the degree of dynamic supercooling, and m is the liquidus slope (dT/dC). The atomic kinetics included the uniform interface motion, layer formation by screw dislocations and by two-dimensional nucleation [29].

3.2. Influence of liquid zone thickness on the growth rate of bulk Si

In our study, the four kinds of liquid zone thickness about 3, 5, 7, 10 mm were chose as shown in Table 1. These samples were placed in same position in the furnace with same holding time for 5 hours. The cross-section photographs of No. 1-4 samples with different alloy thickness and the same temperature gradient of 2.48 K/mm were shown in Fig. 2. It can be found that the MG-Si source was eroded gradually by the alloy melt during the process of TGZM. Meanwhile, the bulk Si grew at the bottom of graphite crucible. The height of bulk Si were approximately 2 mm with the different liquid zone thickness, indicating that the average growth rate of bulk Si was independent on the thickness of liquid zone in our study. The actual growth rates could be expressed as:

$$V_{bulk\ Si} = \frac{H_{bulk\ Si}}{t_{min}} \qquad (2)$$

where $H_{bulk\ Si}$ is the height of the bulk Si (Fig. 2a-d) and t_{min} is 300 min (5 h). The dependence between growth rate and liquid zone thickness determines the change in the contribution of atomic kinetics and diffusion limitations with the increase liquid zone thickness. When the thickness is large, the growth rate is independent of the liquid zone thickness, which indicated that the growth of bulk Si is limited by the diffusion of Si atom in the melt zone. This result is consistent with our research result.
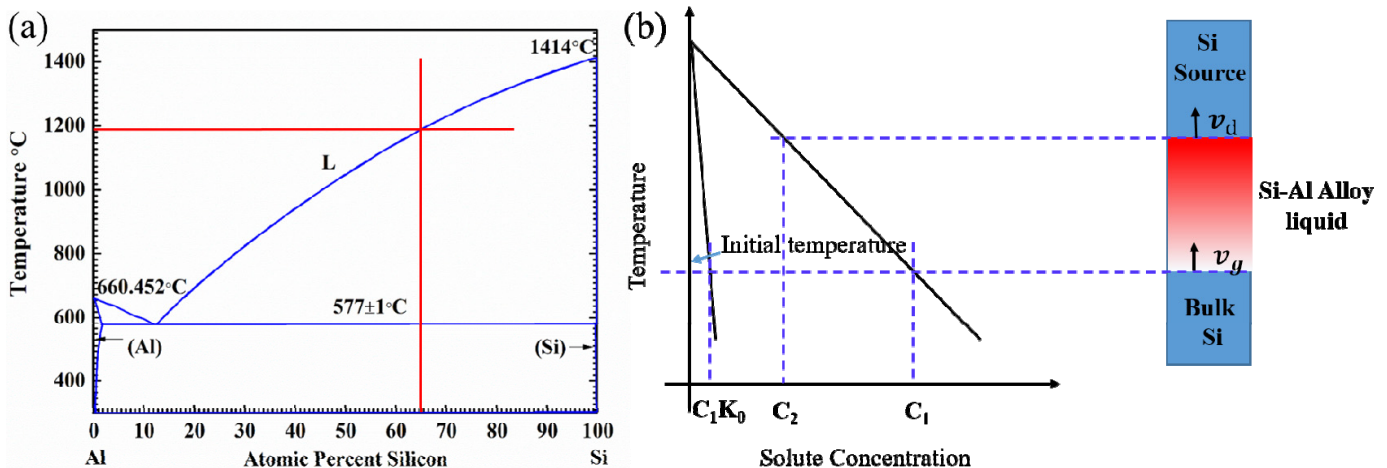

Fig. 1. TGZM schematic diagram

TABLE 1

Sample conditions and results

No.	Alloy Thickness l, mm	Si source Height, mm	Bulk Si Height H, mm
1	3	17	1.79
2	5	17	1.58
3	7	17	2.03
4	10	17	1.57

As shown in cross-section photographs (Fig. 2 a-d), it could be find that the large plates of primary Si were precipitated in the Si-Al alloy melt area. For investigating the precipitate process of primary Si, the different cooling conditions were compared by air atmosphere and water quenching treatment. The samples with the same experiment process (the temperature gradient of 2.48 K/mm) were obtained by the different final cooling method and the microstructure was analyzed and shown in Fig. 3. After the 5 hours holding time finished, the sample (Fig. 3b) was taken out from the furnace immediately and quenching by water. The primary Si was also observed in the Si-Al alloy melt area, which indicated that the primary Si had been precipitated in the TGZM process. Therefore, it also demonstrated that the constitutional supercooling phenomenon had been occurred during the TGZM process. The bulk Si grew at the interface of solid and liquid, besides, the primary Si crystal could also be obtained in the alloy zone. Moreover, it could be found that there was a crack paralleled to the bottom of graphite crucible inside the bulk Si. That was because the bulk Si would generate volume expansion when the melting bulk Si transformed into the solidified bulk Si at the condition of faster cooling.
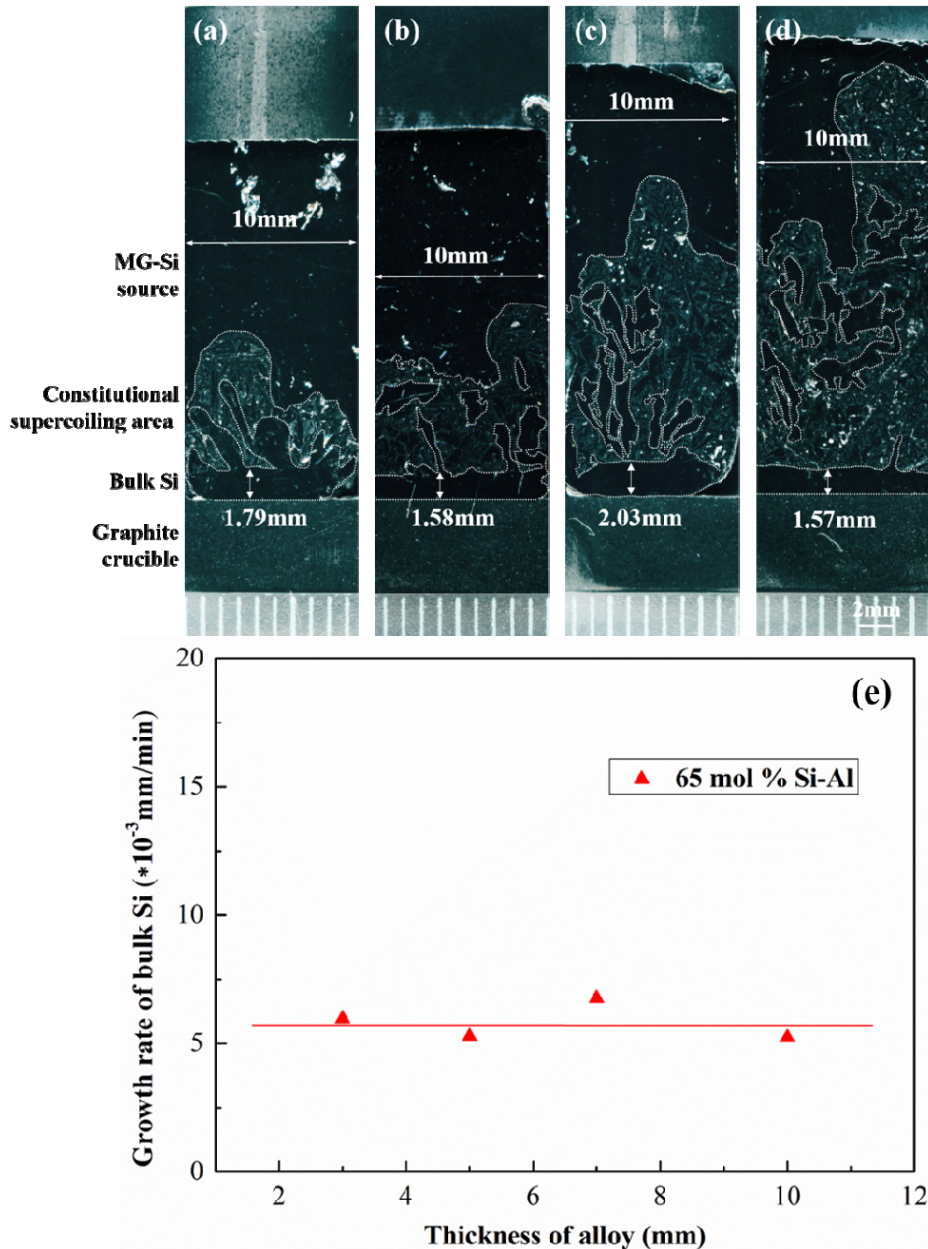

Fig. 2. Cross-section photographs of samples with different alloy thickness and the temperature gradient of 2.48 K/mm; (a) 3 mm; (b) 5 mm; (c) 7 mm; (d) 10 mm; (e) Relationship of growth rate of bulk Si V_g and thickness of liquid zone l
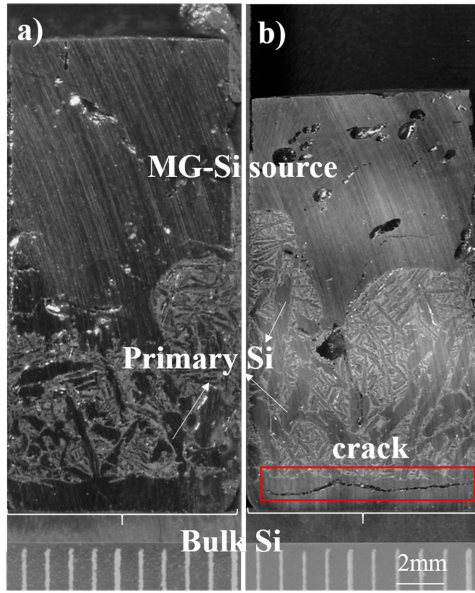
Fig. 3. Cross-section photographs of simples with (a) air cooling; (b) water quenching

Fig. 4. Relationship of growth rate of bulk Si and Al content

3.3. Influence of temperature gradient to growth rate of bulk Si

Usually, for the large thickness of liquid zone l, the growth of crystal at the rate V_g is accompanied by continuous dissolution of source Si (V_d) and motion of liquid Al-Si alloy zone (V) at the same rate. Therefore, the growth rate of the bulk Si is simplified as the following equation [21]:

$$V_g = V_d = V = \frac{GD_L}{mc_L^*(1-k)} \qquad (3)$$

Where c_L^* is the Al initial composition of alloy melt at the interface. It is noted that m is positive, and k is the segregation coefficient between solid/liquid ($k = C_S/C_L$). For the temperature-dependence of diffusion coefficient can be expressed by the Arrhenius Equation [30]:

$$D_L = D_0 \exp(-Q/RT) \qquad (4)$$

Where D_0 is the diffusion coefficient, Q is the diffusion activation energy, R is the gas constant and T is the absolute temperature. The calculated values are listed in Table 2. When the alloy composition is determined, the other parameters are also determined ($D_L = 0.0346$ mm$^2 \cdot$s^{-1}, $m = 829$ k$\cdot$mol%, $c_L^* = 0.350\%$, $k = 0.0028$).

TABLE 2

The activation energy of Al in liquid Si-Al alloy [22]

Element	D_L, mm^2/s	D_0, mm^2/s	Q, J/mol	T, K
Al	0.0346	0.4	29700	1460

In Fig. 4, the theoretical calculation and the experimental values for the growth rate of bulk Si were shown for the different composition and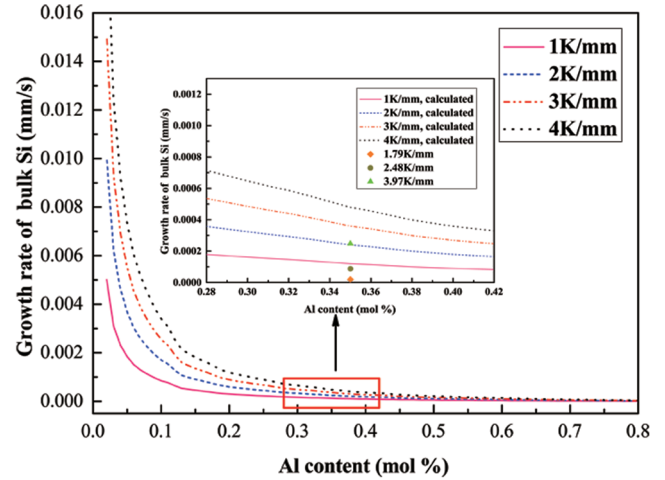 temperature gradients. It was investigated that when the composition of Al was decreased (the composition of Si increased relatively), the theoretical growth rate of bulk Si was promoted. The theoretical calculation values for the growth rate of bulk Si, which were obtained on the base of diffusion limitation mechanism in melt zone, are higher than the experimental values. However, during the experiment process, the formation of constitutional supercooling area and precipitation of primary Si would affect the growth of bulk Si. Meanwhile, large temperature gradient also accelerated the growth of bulk Si. In order to further ensure the relationship of temperature gradient with the growth of bulk Si, more experiments were conducted under the same conditions except the temperature gradients of 1.79, 2.48 and 3.97 K/mm. As shown in Fig. 5, it could be found that while the temperature gradient was 1.79 K/mm (Fig. 5a), there was a little crystal Si precipitated at the bottom and not enough to cover the graphite crucible. Nonetheless, as the temperature gradient was enlarged to 2.48 K/mm, a complete bulk Si covered the bottom of graphite crucible was obtained (Fig. 5b). Moreover, the bulk Si with integrated morphology and about 4.45 mm height was generated when the temperature gradient was increased continually to 3.97 K/mm (Fig. 5c). According to above results, Fig. 5d summarized the relationship between the temperature gradients and the growth rates of bulk Si. It was obvious that the growth rate of bulk Si was positively correlated with the temperature gradients. In the TGZM progress, the temperature gradients has a great influence on the precipitation of primary Si, which determined the growth of bulk Si. It could be also found that with the increase of the temperature gradients, the large plates morphology primary Si crystal (the dark areas) were enriched at the constitutional supercooling area. When the growth rate of bulk Si was lower than the dissolution rate of Si source, the constitutional supercooling area would be formed at the Al-Si alloy zone. Primary Si were precipitated and grown in the liquid melting during the growth of bulk Si. The precipitation of primary Si had occurred during the whole process of the growth of bulk Si, which had been described in the following part. The inclusions and eutectic structure (the light areas) reduced continuously in constitutional supercooling area.
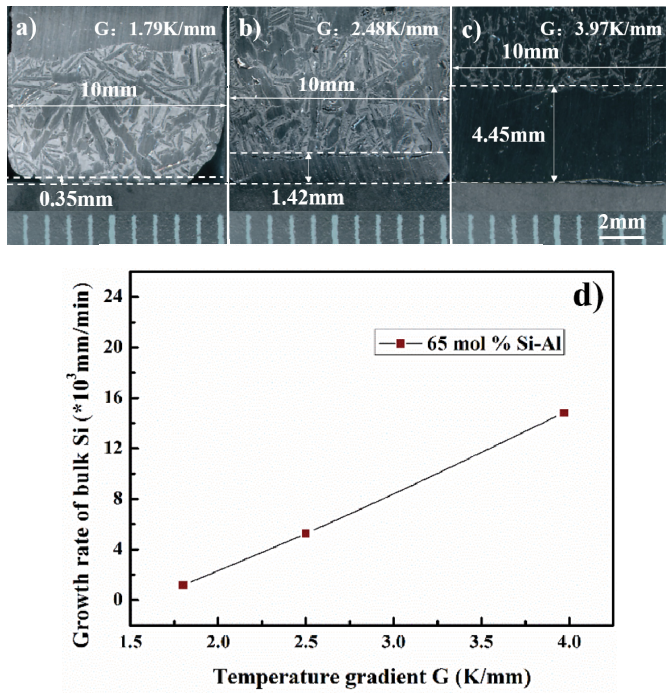
Fig. 5. Cross-section photographs of samples with different temperature gradient; (a) 1.79 K / mm; (b) 2.48 K / mm; (c) 3.97 K / mm; (d) Relation curve of temperature gradient and growth rate of bulk Si

3.4. Influence of holding time on the macrostructure of bulk Si

Fig. 6 showed the vertical sections of samples under different holding time. It could be found that there was a little primary Si crystal at the bottom center and not enough to cover the graphite crucible with some hole defects for 1 hour holding time (Fig. 6a). However, it illustrated that the bulk Si grew at the beginning of the TGZM. After 3 h holding time (Fig. 6b), the bulk Si with a rough growth interface was obtained. When the holding time was further prolonged to 5 h, a bulk Si with a smooth solid-liquid interface was present at the bottom of the sample. As shown in Fig. 6c, no cracks and inclusions were detected in the bulk Si.

Moreover, to further illustrate the continuous growth of bulk Si, Fig. 6d shows the relationship of holding time and the height of bulk Si. It could be found that the height of bulk Si was linear with the holding time, which can indicate that the bulk Si grew with a constant rate in the range of holding time of 1-5 hours. Meanwhile, it demonstrated that the bulk Si grew from beginning to end of the whole TGZM process and had not been interrupted.

In addition, when Si source was dissolved and diffused into the alloy melt, abundant impurities were expelled into the alloy melt, which leaded the phenomenon that constitutional supercooling occurred. With the increase of holding time, the constitutional undercooling became rapidly severe. In this case, a mass of MG-Si was supplied as the source so that there were many redundant source Si at the top of samples.
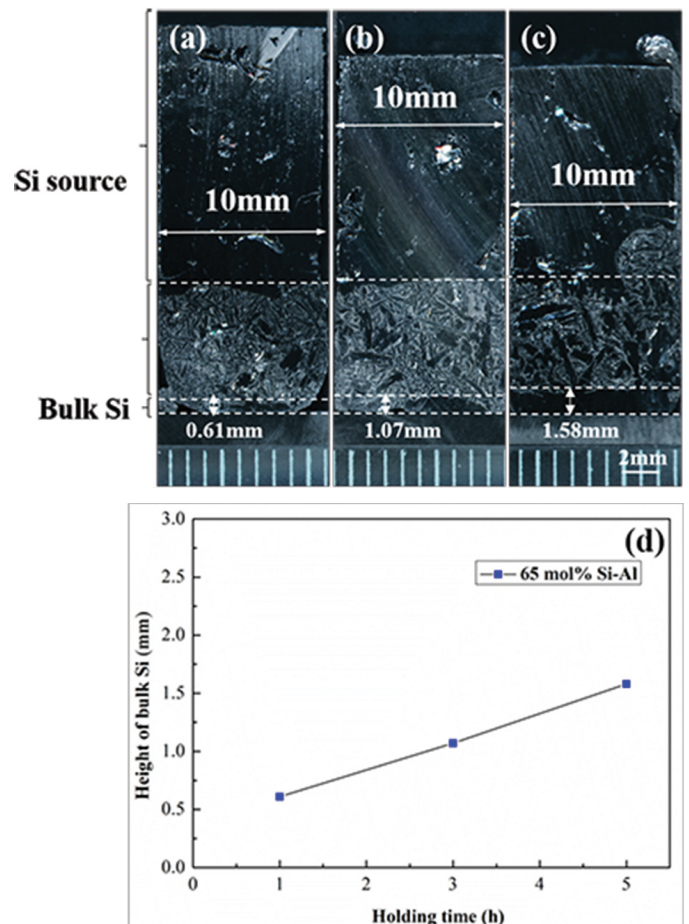

Fig. 6. Vertical cross-sections of samples with different holding time; (a) 1 hour; (b) 3 hours; (c) 5 hours; (d) The relation curve of holding time and height of bulk Si

3.5. Impurities

Fig. 7 shown the distribution of impurities at the interface of the bulk Si and the constitutional supercoiling area detected by EPMA element mapping analysis in Fig. 2b. It could be found that the gray area (marked primary Si and bulk Si area) was main Si element (Fig. 7c) and Al, Fe and B elements existed hardly at this region. But the Al element was mainly gathered at the dark area (marked Al-Si eutectic) as well as some Si element. Besides, those white inclusions (Fig. 7a) were mainly Fe impurity distributing at the Al-Si eutectic area. In short, the Al and some other impurities were stuck in the Al-Si eutectic structure after the TGZM process, in this way purified primary Si and the bulk Si were obtained.

In order to further confirm the impurity distribution at the bulk, primary Si and eutectic structure, the line analysis of Si, B, Al and Fe elements from the Al-Si eutectic to the bulk Si was done by EPMA in Fig. 8. It could be discovered that most of the iron also was segregated into the Al-Si eutectic. The boron could not be detected by EPMA line analysis due to the low content.

Table 3 showed the impurities contents of the MG-Si source and the bulk Si at the temperature gradient of 2.48 K/mm and 3.97 K/mm (Fig. 5b and Fig. 5c) detected by the ICP-MS. Compared
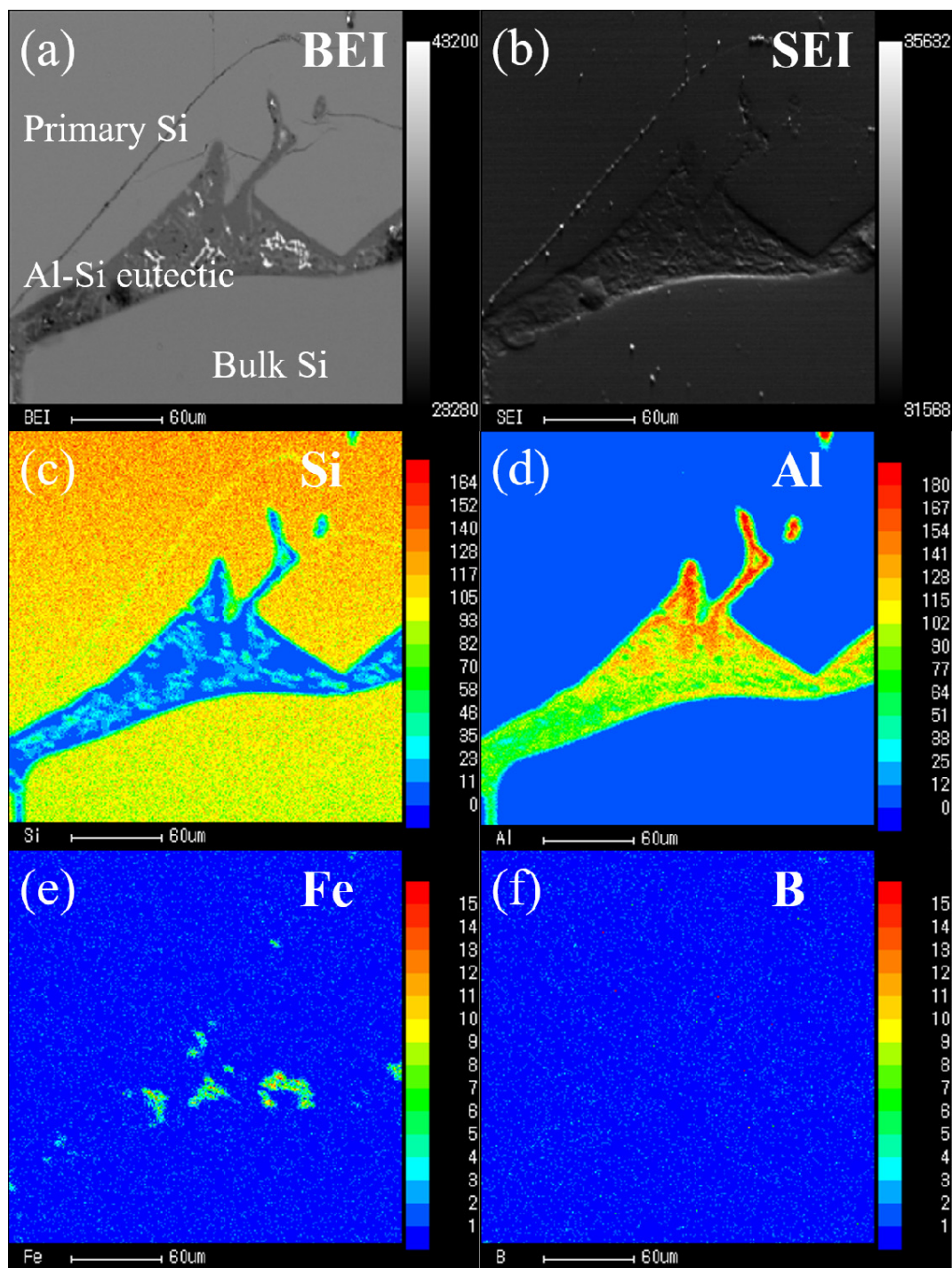
Fig. 7. Image of the interface of bulk Si, Al-Si eutectic and primary Si (a) BEI; (b) SEI; EPMA element mapping analysis for (c) Si, (d) Al, (e) Fe and (f) B element

TABLE 3

Impurities contents of the MG-Si source and the bulk Si

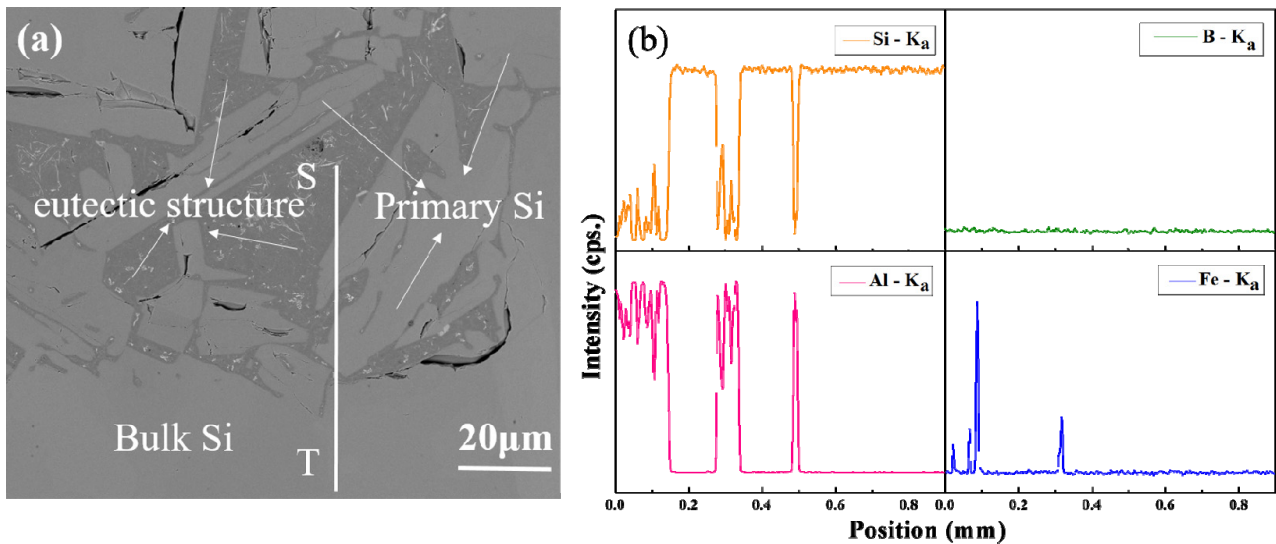| Imputities	Fe	B	P	Al	V	Mg	Ti	Cu
Bulk Si-1	2.26	5.15	0.92	238.73	0.21	0.24	0.32	0.06
Bulk Si-2	5.33	7.38	10.02	488.43	0.77	0.21	0.92	0.18
MG-Si source	1106.85	14.14	15.25	673.01	202.34	0.84	239.51	20.83
Imputities	Ni	Cr	Mn	Ga	As	Sn	Ca	Na
Bulk Si-1	0.22	0.02	0.08	<0.006	<0.006	0.02	<0.30	<0.30
Bulk Si-2	0.36	0.04	0.27	0.01	0.03	0.02	1.00	0.74
MG-Si source	42.5	2.77	<0.60	1.93	<0.60	<0.60	49.52	0.82

(Unit: ppmw)

Fig. 8. Image of the interface of bulk Si, Al-Si eutectic and primary Si (a) SEM; (b) Line analysis of Si, B, Al and Fe in Fig. 2 b

with the content of impurities of MG-Si source, most of the impurities such as Fe, B, P and so on were reduced dramatically in the bulk Si obtained by the TGZM method. Obviously, with different temperature gradients, the removal fractions of impurities were different. At the temperature gradient of 2.48 K/mm (Bulk Si-1), the removal rates of Fe, P and B were 99.8%, 94.0%, and 63.6%, respectively. However, when the temperature gradient was increased to 3.97 K/mm (Bulk Si-2), the removal efficiency of impurities was weaken and the contents of impurities of the bulk Si were increased, compared to the temperature gradient of 2.48 K/mm. It proved that Si-Al alloy had a more effective segregation effect on the majority of the impurities at the lower refining temperature.

4. Conclusions

The bulk Si, which grew continuously in the 65 mol.% Si-Al alloy used TGZM method, was investigated. The results indicated that the growth rate of bulk Si was independence of the liquid zone thickness l in our study. And when the temperature gradient was changed from 2.48 K/mm to 3.97 K/mm, the growth rate of the bulk Si was enhanced from 7.9×10^{-5} mm/s to 2.47×10^{-4} mm/s which was increased by 3 times approximately. As the Si source remained, the bulk Si would grow unceasingly during prolonging the holding time from 1 h to 5 h. Moreover, low refining temperature was particularly beneficial to the removal of impurities. With the precipitation temperature of 1460 K and the temperature gradient of 2.48 K/mm, the removal rates of Fe, P and B were 99.8%, 94.0% and 63.6%, respectively.

REFERENCES

[1] J. Chung, J. Kim, B. Jang, Y. Ahn, H. Lee, W. Yoon, Sol. Energ. Mat. Sol. C. **95** (1), 45-48 (2011).

[2] S. Esfahani, M. Barati, Met. Mater. Int. **17** (6), 1009-1015 (2011).

[3] L.K. Jakobsson, M. Tangstad, Metall. Mater. Trans. A **46** (2), 595-605 (2015).

[4] L.T. Khajavi, K. Morita, T. Yoshikawa, M. Barati, J. Alloy. Compd. **619**, 634-638(2015).

[5] J.W. Li, Z. Guo, J. Cryst. Growth. **394** (10), 18-23(2014).

[6] T. Yoshikawa, K. Morita, J. Cryst. Growth. **311** (3), 776-779 (2009).

[7] J.Y. Li, P. Ni, L. Wang, Y. Tan, Mat. Sci. Semicon. Proc. **61**, 79-84 (2017).

[8] T. Yoshikawa, K. Morita, S. Kawanishi, et al, J. Alloy. Compd. **490** (1-2), 31-41 (2010).

[9] T. Yoshikawa, K. Morita, Sci. Technol. Adv. Mat. **4** (6), 531-537 (2003).

[10] T. Yoshikawa, K. Morita. ISIJ Int. **45** (7), 967-971 (2005).

[11] T. Yoshikawa, K. Morita. J. Cryst. Growth. **311** (3), 776-779 (2009).

[12] Y.Q. Li, Y. Tan, P.P. Cao, J. Li, P.J. Jia, Y. Liu, Mater. Res. Innov. **19** (2), 81-85 (2015).

[13] H.F. Lu, K.X Wei, W.H. Ma. K.Q. Xie, J.J. Wu, Y. Lei, Y.N. Dai, Mater. Rev. **29** (8A), 90-97 (2015).

[14] L.Q. Huang, H.X. Lai, C.H. Lu, M. Fang, W.H. Ma, P.F. Xing, J.T. Li, X.T. Luo Hydrometallurgy **161**, 14-21(2016).

[15] Q.C. Zou, J.C. Jie, T.M. Wang, T.J. Li, Mater. Lett. **185**, 59-62 (2016).

[16] T. Yoshikawa, K. Morita, ISIJ. Int. **47** (4), 582-584 (2007).

[17] Y.H. Zhang, X.C. Miao, Z.Y. Shen, Q.Y. Han, C.J. Song, Q.J. Zhai, Acta. Mater. 97, 357-366 (2015).

[18] J.W. Li, Z.C. Guo, J.C. Li, L.Z. Yu, Silicon. **7** (3), 1-8 (2014).

[19] X. Gu, X. Yu, D. Yang, Sep. Purif. Technol. **77** (1), 33-39 (2011).

[20] J. Chung, C. Lee, J. Lee, W. Yoon, Sep. Sci. Technol. **48** (15), 2345-23514 (2013).

278

[21] P. P. Wang, H. M. Lu, Y. S. Lai, J. Cryst. Growth. **390**, 96-100 (2014).

[22] Y. Nishi, Y. Kang, K. Morita, Mater. Trans. **51** (7), 1227-1230 (2010).

[23] X. D. Ma, T. Yoshikawa, K. Morita, J. Cryst. Growth**. 377** (2013), 192-196.

[24] L. F. Zhang, Y. S. Ma, Y. Q. Li. Mat. Sci. Semicon. Proc. **71**, 12-19 (2017).

[25] W.G. Pfann, A. Chem, Anal. Chem. **36** (12), 2231-2234 (1964).

[26] V.N. Lozovskii, V.P. Popov, Prog. Cryst. Growth & Charact. **6**, 1-23(1983).

[27] J.Y. Li, L. Wang, P. Ni, Y. Tan. Mat. Sci. Semicon. Proc. **66**, 170-175 (2017).

[28] W.A. Tiller, J. Appl. Phys. **34** (9), 2757-2762 (1963).

[29] Z. Ebrahimi, Arch. Metall. & Mater. **62** (4), 1969-1981 (2017).

[30] H.E. Cline, T.R. Anthony, J. Appl. Phys. **43**, 4391-4395 (1972).